ISBN: 978-3-95450-247-9 ISSN: 2673-5490 doi: 10.18429/JACoW-IPAC2024-TUPC76

OPTIMIZATIONS AND UPDATES OF THE FCC-ee COLLIMATION SYSTEM DESIGN

G. Broggi[1,2,3,*], A. Abramov[3], K. André[3], M. Boscolo[2], R. Bruce[3], M. Hofer[3], S. Redaelli[3]
[1]Sapienza University of Rome, Italy, [2]INFN-LNF, Frascati, Italy, [3]CERN, Meyrin, Switzerland

Abstract

The Future Circular electron-positron Collider, FCC-ee, is a design study for a 90.7 km circumference luminosity-frontier and highest-energy e^+e^- collider. It foresees four operation modes optimized for producing different particles by colliding high-brightness lepton beams. Operating such a machine presents unique challenges, including the handling of stored beam energies up to 17.5 MJ, a value about two orders of magnitude higher than any lepton collider to date. Given this stored beam energy, unavoidable beam losses pose a serious risk of damage. To address this challenge, a beam collimation system is required to protect the sensitive equipment of this machine. This paper presents the current FCC-ee collimation system baseline and a collimation performance evaluation under selected beam loss scenarios.

INTRODUCTION

The FCC-ee [1, 2], a synchrotron with approximately 90.7 km circumference, is being designed as a possible luminosity-frontier and highest-energy e^+e^- collider. It foresees four operation modes, with beam energies of 45.6 GeV, 80 GeV, 120 GeV and 182.5 GeV, optimized for producing different particles (Z, W, H, $t\bar{t}$). The FCC-ee layout considered in this work [2] includes four interaction points (IPA, IPD, IPG, IPJ) and four straight sections (PB, PF, PH, PL). Given the stored beam energy, reaching 17.5 MJ in the Z mode, the FCC-ee beams have a critical damage potential. Therefore, a collimation system is indispensable, not only to reduce backgrounds in the detectors, as in any lepton collider to date, but also to protect sensitive machine components, from beam losses that will unavoidably occur during operation. In this article, we present the status of the FCC-ee collimation studies, including a collimation performance evaluation for the latest machine and collimation system baseline under selected beam loss scenarios. The latest optimization studies for the halo collimator length are presented in the last section.

FCC-ee COLLIMATION SYSTEM

The FCC-ee collimation system has two main roles: protecting the sensitive machine equipment from unavoidable beam losses and reducing the background in the experiments. To address these challenges, a beam halo (or global) collimation system is foreseen to be installed in the PF insertion [3–8], as well as synchrotron radiation (SR) collimation upstream of each IP. This article is focused on the halo collimation system. Details on the FCC-ee SR collimation are reported in Ref. [9]. The halo collimation system includes both a system for betatron (β) and off-momentum (δ) losses. The current halo collimator design consists of 25 cm long molybdenum carbide-graphite (MoGr) primary collimators (TCPs) and 30 cm long molybdenum secondary collimators (TCSs). These preliminary design parameters were selected based on considerations aiming to achieve a good balance between material robustness, thermal stability, impedance, and collimation efficiency [5, 7, 10]. Research and development on collimator material candidates is ongoing [2], and the choice of materials will be refined in the future as the FCC-ee design advances. The parameters and settings for the current halo collimation system baseline are summarized in Table 1. The δ collimator settings were determined relying on linear dispersion only. Future studies will encompass higher-order dispersion, as recent findings have shown its importance for large momentum offsets.

Table 1: FCC-ee (Z) Halo Collimator Parameters

Type (#)	Plane	Material	Length [m]	Half-gap [σ (mm)]	δ_{cut} [%]
β prim. (1)	H	MoGr	0.25	11.0 (6.7)	8.9
β sec. (2)	H	Mo	0.3	13.0 (3.8, 5.1)	6.7, 90.6
β prim. (1)	V	MoGr	0.25	65.0 (2.4)	–
β sec. (2)	V	Mo	0.3	75.0 (2.5, 2.9)	–
δ prim. (1)	H	MoGr	0.25	18.5 (4.2)	1.3
δ sec. (2)	H	Mo	0.3	21.5 (4.6, 16.7)	2.1, 1.6

COLLIMATION INSERTION OPTICS

A dedicated optics for the halo collimation insertion in PF has been designed for FCC-ee optics V23 [11, 12], see Fig. 1. The PF optics is based on three sets of quadrupole doublets and allows combining betatron and off-momentum collimation in one single insertion while maintaining optimal collimator phase advances and acceptable mechanical gaps for impedance constraints. The optimal TCP-to-TCS phase advances μ are given by $\mu = \tan^{-1}\left(\frac{\sqrt{n_2^2-n_1^2}}{n_1}\right)$, with n_1 and n_2 being the TCP and TCS openings in units of RMS beam size [13]. For betatron cleaning, small Twiss α-functions at the β-TCPs, rather than tilted collimators, are used to ensure that particles hit the jaws parallel to the surface to maximize the effective collimator active length [6, 7, 10].

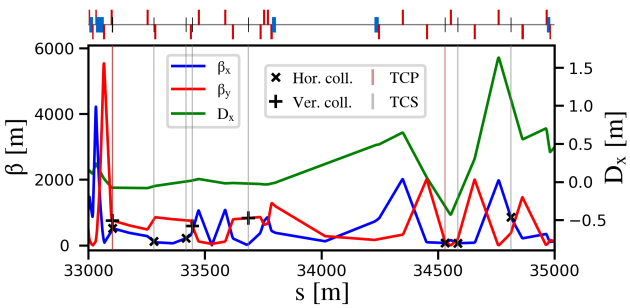

Figure 1: FCC-ee collimation insertion (PF) optics.

* giacomo.broggi@cern.ch

ISBN: 978-3-95450-247-9 ISSN: 2673-5490 doi: 10.18429/JACoW-IPAC2024-TUPC76

SIMULATION SETUP

The FCC-ee halo collimation performance is evaluated using the Xsuite-BDSIM simulation tool [8, 14–19], which combines particle tracking in the magnetic lattice and particle-matter interactions in the collimators. For the studies in this paper, the positron beam (B1) with 45.6 GeV beam energy (FCC-ee Z) is simulated. This is the most critical machine mode for stored beam energy. Simulations are done for horizontal betatron halo (B1H) and off-momentum (B1-dp) collimation. A generic beam halo loss is studied, with the starting beam distribution sampled at the impacted TCP so that all the particles interact with it on the first pass. Two distribution sampling methods are adopted: the first, referred to as *point halo*, returns a point-like matched beam at a given transverse depth from the collimator edge (or *impact parameter, b*). The second, referred to as *direct halo*, returns a matched beam distribution that extends from the collimator edge up to a *maximum impact parameter*, $b_{\max}$, as in [20]. The studies performed to date [6, 21] adopted the point halo method. Such a method, despite being unrealistic as the beam transverse profile continuously extends from the beam core to the tails, aims to provide a pessimistic estimate of the collimation performance by making all the particles impact at the *critical impact parameter* b_{crit}, i.e., the one leading to the worse collimation performance. However, impact parameter scans performed with the present collimation layout and optics did not show any b_{crit}, with monotonically worsening collimation performance observed when going towards smaller impact parameters [22]. Therefore, we decided to extend our studies by including the direct halo method, which provides a more realistic modelling of the collimation process. For the point halo method $b = 1$ µm is considered, as in previous studies. For the direct halo method, $b_{max} = 1$ µm is used, aiming to cover all the impact parameters in the range $[0, b_{max}]$. In each simulation, 5×10^6 primary particles are tracked for 700 turns, including the effects of SR, radiofrequency cavities and magnetic lattice tapering. The beam loss positions are recorded and their distribution along s is binned in 10 cm intervals to produce loss maps in terms of the local cleaning inefficiency $\eta = E_{\text{loss},\Delta s}/(E_{\text{loss,tot}}\Delta s)$, with $E_{\text{loss},\Delta s}$ being the integrated energy of particles lost in $[s, s + \Delta s]$ and $E_{\text{loss,tot}}$ the integrated energy lost over the whole ring. For the off-momentum case, the beam is sampled on one of the δ-TCP jaws, corresponding to particles with negative momentum deviation ($-dp$) and no betatron amplitude. The δ-TCP is aligned to the divergence of the dispersive trajectory, $x' = D'_x \delta_c$, with δ_c being the momentum cut of the δ-TCP, by applying a tilt of 63 µrad. Otherwise the large angle of incidence would significantly reduce the effective δ-TCP active length [10].

RESULTS

The loss maps for the full FCC-ee ring are shown in Fig. 2, for the different studied halos. It is clear that in the case of betatron losses on β-TCPs, the outscattered particles not intercepted by the TCSs are lost over the whole ring, and

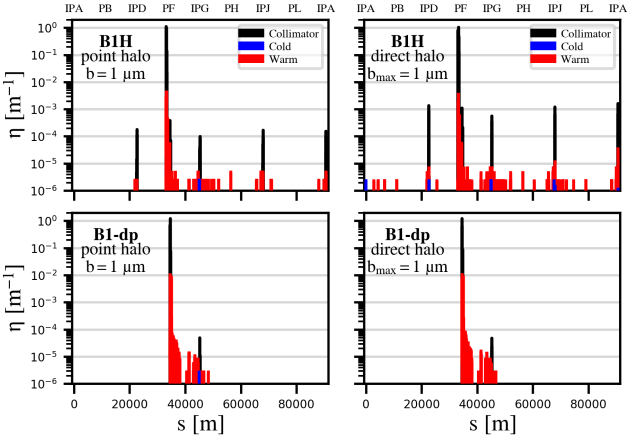

Figure 2: FCC-ee (Z) beam halo loss maps: β-horizontal (top) and off-momentum with tilted δ-TCP (bottom), adopting *point halo* (left) and *direct halo* (right) methods.

in particular close to all four IPs. It is also evident that the betatron collimation performance worsens in the direct halo case, consistently with previous impact parameter scan studies [22]. Therefore, from now on, we use this method for our evaluations, aiming to provide collimation performance estimates that are sufficiently conservative. In this scenario, the collimation system is anyway capable of absorbing the vast majority of the losses, with >99.65% of all losses confined in the collimation insertion PF for all the simulated cases. Assessing the beam power loss at 5 min lifetime, up to 41 W out of the total power loss of 58.3 kW are found in the regions ±120 m from the IPs, which is critical for backgrounds [23]. In the off-momentum case, the configuration with the δ-TCP aligned to the dispersive trajectory shows a good performance, with all particles stopped on the first turn and no losses beyond IPG. It should be noted that for the case with the δ-TCP parallel to the on-momentum closed orbit and considering the same b_{max}, the integrated losses downstream of IPG reach 2.2 kW. Therefore, the angular alignment of the collimator has a crucial effect on off-momentum losses. The collimation performance in the betatron case is sufficiently good with untilted collimator jaws. This is because the divergence of the beam envelope at the β-TCPs is rather small (14 µrad for B1H) when compared to the tilt of the δ-TCP. The simulations show that SR collimators upstream of the IPs play a crucial role in protecting the aperture bottlenecks in the interaction regions (IRs), since they intercept sizeable losses that would otherwise hit the final-focus superconducting quadrupoles. The SR collimators were, however, primarily designed to reduce photon background from SR emission rather than to absorb beam losses. It is therefore crucial to ensure that the total power loads on these devices remain below the material damage threshold. In the studies presented here the maximum recorded power load on any SR collimator is only around 8.2 W (in IPA, for B1H), see Fig. 3. This value is much lower than the maximum recorded power load from SR of about 200 W [9]. In general, the power loads on elements outside of the collimation insertion are at most of the order

ISBN: 978-3-95450-247-9 ISSN: 2673-5490 doi: 10.18429/JACoW-IPAC2024-TUPC76

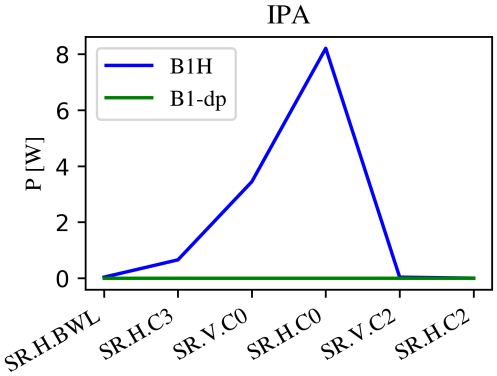

Figure 3: Power loads from collimation losses on SR collimators upstream of the most exposed IP (IPA).

of 10 W. This is probably sufficiently low, although local energy deposition studies and detailed assessments of the tolerance to beam losses are needed to quantitatively assess the effect of the losses on the impacted and downstream elements. However, the power load may be higher in other scenarios with smaller impact parameters, which should be studied in the future.

COLLIMATOR LENGTH OPTIMIZATION

Collimators, by introducing geometric and material discontinuities in the beam path, significantly contribute to impedance, potentially affecting the beam stability [24, 25]. With the high stored beam energy at the FCC-ee, robustness is a key aspect for collimator design, especially for TCPs, typically constructed from materials like graphite or its derivatives (e.g., MoGr) [26, 27]. These materials typically exhibit relatively low electrical conductivity, thus further amplifying their impedance contribution. Therefore, it is important to find an equilibrium between collimation performance, robustness and impedance. Given that the collimator contribution to the resistive wall impedance scales linearly with the length, we conducted parametric studies of the cleaning performance with varying length of TCPs and TCSs, aiming at reducing impedance. These studies consisted of direct halo collimation simulations as described in the previous sections. The chosen figure of merit for collimation performance is the cumulative power load within $\pm$120 m from each IP (P_{IRs}). Results for the TCP length (L_{TCP}) scan are depicted in Fig. 4.

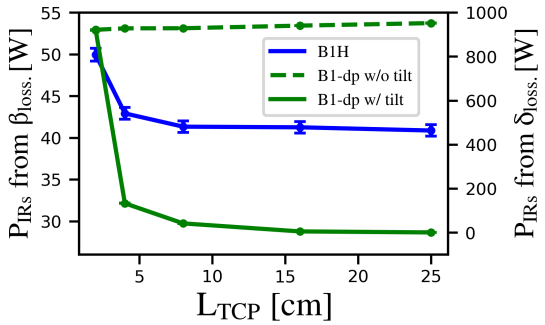

Figure 4: Collimation performance as a function of L_{TCP}.

Fig. 4 illustrates that, in case of betatron losses ($\beta_{loss.}$) the collimation performance remains practically unchanged down to L_{TCP} = 4 cm. Below this length, an increase in P_{IRs} of 20% is observed, with a peak power load of 9 W on the horizontal SR collimator SR.H.C0 upstream of IPA. This is consistent with previous findings [10] as well as with the average effective collimator active length of approximately 4 cm for particles impacting the horizontal β-TCP with 14 µrad angle and impact parameter within [0,b_{max}]. For off-momentum losses ($\delta_{loss.}$), it is evident, once again, that the collimation performance increases when aligning the δ-TCP to the dispersive trajectory, with a P_{IRs} suppression >87.5% until L_{TCP} = 4 cm. However, such suppression capability vanishes at L_{TCP} = 2 cm as the δ-TCP length approaches the average effective collimator active length of about 1 cm for off-momentum particles impacting the δ-TCP with 64 µrad angle and impact parameter within [0,b_{max}]. A scan of the TCS length, L_{TCS}, showed that in the betatron case, the performance remains unchanged even at very short L_{TCS} (1 cm), while in the off-momentum case, performance slightly worsens with shorter L_{TCS}. Such observations indicate a large potential for shortening the TCSs, thereby greatly improving impedance. It should be mentioned that our current assumption on L_{TCS}, which requires the complete stopping of 182.5 GeV (FCC-ee $t\bar{t}$ energy) $e^{\pm}$ normally incident on the collimator edge [5], was deliberately stringent and conservative, aiming to allow for optimization in later design stages. Additionally, the material currently assumed for TCSs, Mo, has a relatively high Z and short radiation length ($\simeq$1cm), differing from the more robust materials currently assumed for TCPs. This contrast in material properties may explain the observed non-sensitivity of the collimation performance to the L_{TCS}, as the high stopping power of Mo can ensure effective cleaning even with a very small amount of material.

CONCLUSIONS AND OUTLOOK

Our study presented a comprehensive analysis of the FCC-ee collimation system, focusing on the halo collimation performance with the latest layout and after halo collimator optimization efforts. Through an extensive simulation campaign, we evaluated the performance of the current collimation system baseline in mitigating generic beam halo losses. Our findings demonstrate the effectiveness of the collimation system in confining beam losses within designated regions and highlight the importance of alignment between collimators and optics for optimal performance. Our analysis also shows promising potential for improving impedance by reducing the halo collimator length. Our simulations currently assume a maximum impact parameter of 1 µm, and further studies are required to determine the most realistic value. These forthcoming investigations, including simulations of various beam-halo formation processes, like beam-gas or Touschek scattering, hold significant promise for refining our simulation model and further optimizing the FCC-ee collimation system.

ISBN: 978-3-95450-247-9 ISSN: 2673-5490 doi: 10.18429/JACoW-IPAC2024-TUPC76

REFERENCES

[1] A. Abada *et al.*, "FCC-ee: The Lepton Collider," *Eur. Phys. J. Spec. Top.*, vol. 228, no. 2, 2019, pp. 261–623.

[2] B. Auchmann *et al.*, "FCC Midterm Report," *CERN Report*, 2024.

[3] A. Abramov, *et al.*, "Development of collimation simulations for the FCC-ee," in *Proc. IPAC'22*, Bangkok, Thailand, June 2022, paper WEPOST016, pp. 1718–1721. doi:10.18429/JACoW-IPAC2022-WEPOST016

[4] M. Hofer, *et al.*, "Design of a collimation section for the FCC-ee," in *Proc. IPAC'22*, Bangkok, Thailand, June 2022, paper WEPOST017, pp. 1722–1725. doi:10.18429/JACoW-IPAC2022-WEPOST017

[5] G. Broggi, "First study of collimator design for the FCC-ee," Master's thesis, Politecnico di Milano, 2022.

[6] A. Abramov, *et al.*, "Studies of layout and cleaning performance for the FCC-ee collimation system," in *Proc. IPAC'23*, Venice, Italy, May 2023, paper MOPA128, pp. 356–359. doi:10.18429/JACoW-IPAC2023-MOPA128

[7] G. Broggi, A. Abramov, R. Bruce, "Beam dynamics studies for the FCC-ee collimation system design," in *Proc. IPAC'23*, Venice, Italy, May 2023, paper MOPA129, pp. 360–363. doi:10.18429/JACoW-IPAC2023-MOPA129

[8] A. Abramov, *et al.*, "Collimation simulations for the FCC-ee," *J. Instrum.*, vol. 19, p. T02004, 2024. doi:10.1088/1748-0221/19/02/T02004

[9] K. André, *et al.*, "Status of the synchrotron radiation studies in the interaction region of the FCC-ee," presented at IPAC'24, Nashville, TN, USA, May 2024, paper WEPR09, this conference.

[10] G. Broggi, "Tracking studies for the FCC-ee collimation system design," submitted for publication to *Il Nuovo Cimento – Colloquia and communications in physics*, 2024.

[11] M. Hofer, "FCC-ee collimation lattice," GitLab repository, https://gitlab.cern.ch/mihofer/fcc-ee-collimation-lattice

[12] K. Oide, "FCC-ee collider optics," presented at FCC week 2023, London, UK, June 2023.

[13] J.B. Jeanneret, "Optics of a two-stage collimation system," *Phys. Rev. Spec. Top. Accel. Beams*, vol. 1, p. 081001, 1998. doi:10.1103/PhysRevSTAB.1.081001

[14] G. Iadarola, *et al.*, "Xsuite: an integrated beam physics simulation framework," in *Proc. HB'23*, Geneva, Switzerland, Oct. 2023, paper TUA2I1. doi:10.18429/JACoW-HB2023-TUA2I1

[15] L. Nevay, *et al.*, "BDSIM: An accelerator tracking code with particle–matter interactions," *Comput. Phys. Commun.*, vol. 252, p. 107200, 2020. doi:10.1016/j.cpc.2020.107200

[16] L. Nevay, *et al.*, "BDSIM: Automatic Geant4 Models of Accelerators," in *Proc. ICFA Mini-Workshop on Tracking for Collimation*, CERN, Geneva, Switzerland, p. 45, 2018. doi:10.23732/CYRCP-2018-002.45

[17] J. Allison, *et al.*, "Recent developments in Geant4," *Nucl. Instrum. Methods. Phys. Res., Sect. B*, vol. 835, pp. 186–225, 2016. doi:10.1016/j.nima.2016.06.125

[18] S. Agostinelli, *et al.*, "Geant4—a simulation toolkit," *Nucl. Instrum. Methods. Phys. Res., Sect. A*, vol. 506, pp. 250–303, 2003. doi:10.1016/S0168-9002(03)01368-8

[19] J. Allison, *et al.*, "Geant4 developments and applications," *IEEE Trans. Nucl. Sci.*, vol. 53, pp. 270–278, 2006. doi:10.1109/TNS.2006.869826

[20] R. Bruce, *et al.*, "Simulations and measurements of beam loss patterns at the CERN Large Hadron Collider," *Phys. Rev. Spec. Top. Accel. Beams*, vol. 17, p. 081004, 2014. doi:10.1103/PhysRevSTAB.17.081004

[21] G. Broggi, "FCC-ee collimation status," presented at FCCIS WP2 Workshop, Rome, Italy, November 2023.

[22] G. Broggi, "IR beam losses and collimation status," presented at FCC-ee MDI & IR mockup workshop, Frascati, Italy, November 2023.

[23] M. Boscolo, *et al.*, "Progress in the design of the Future Circular Collider FCC-ee interaction region," presented at IPAC'24, Nashville, Tennessee, USA, May 2024, paper TUPC67, this conference.

[24] M. Migliorati, *et al.*, "Studies of FCC-ee single bunch instabilities with an updated impedance model," *J. Phys.: Conf. Ser.*, vol. 2687, p. 062010, 2024. doi:10.1088/1742-6596/2687/6/062010

[25] M. Behtouei, *et al.*, "Wakefields excited in the FCC-ee collimation system," *J. Instrum.*, vol. 19, p. P02014, 2024. doi:10.1088/1748-0221/19/02/P02014

[26] C. Accettura, *et al.*, "Overview of material choices for HL-LHC collimators," *J. Phys.: Conf. Ser.*, vol. 2687, p. 062010, 2024. doi:10.1088/1742-6596/2687/6/062010

[27] S. Terui, *et al.*, "Low-Z collimator for SuperKEKB," *Nucl. Instrum. Methods Phys. Res., Sect. A*, vol. 1047, p. 167857, 2023. doi:10.1016/j.nima.2022.167857